Histological evaluation of tissue damage caused by bioinspired needle insertion

M. Sahlabadi[1], S.T.R. Gidde[1], P. Gehret[2], K. Esmaeili Pourfarhangi[2], B. Bayarmagnai[2], and P. Hutapea[1]*

[1] Department of Mechanical Engineering, Temple University, Philadelphia, PA 19122 USA
[2] Department of Bioengineering, Temple University, Philadelphia, PA 19122 USA

A novel bioinspired design for surgical needles was proposed in our previous work which reduces insertion and extraction forces during needle-based procedures. The results obtained from insertion and extraction tests into artificial and biological tissues showed 35–45% reduction in the insertion force, and 15–20% reduction in the extraction force using bioinspired needles. From literature, it has been known that reducing needle forces results in less invasive medical procedure. In this paper, a histological study was conducted to accurately measure the tissue damage caused by needles to tissue. The insertion tests into bovine liver tissue were performed using bioinspired and conventional needles. Liver tissue samples were fixed and sectioned into slices with the thickness of 0.08 ìm and stained using hematoxylin and eosin staining method to enhance visualization of the cells. The results obtained from the histological study showed that the tissue damage was decreased by 31% using bioinspired needle. The results obtained from the histological study strongly supports our previous assumption that reducing needle's forces and the tissue deformation during an insertion results in less tissue damage. Therefore, the proposed bioinspired design can be implemented to design surgical needles which are more accurate and less invasive.

Keywords: histological study, tissue damage, bioinspired design, honeybee, medical devices, insertion force

DOI 10.24411/2409-2568-2018-10001

1. Introduction

Needle-based procedures can cause significant damages to soft tissues. Therefore, in recent years, there has been a growing interest among medical community to make needle-based procedures less invasive. Needles are used in medical procedures for different purposes such as drug delivery, biopsy, cancer treatment (through brachytherapy or thermal ablation), brain imaging, and deep brain stimulation. To make needle-based procedure more effective and less invasive, the insertion mechanics of the needle needs to be studied. The effective factors in a needle insertion are the geometry of needle (body and tip's geometries) [1–4], the material properties of tissue [5–10], the dynamics of insertion (i.e., insertion with rotation and/or vibration) [11–16], and the speed of needle's insertion or extraction [17, 18].

Gerwen et al. [5] reported that reducing forces acting on needle body will reduce the tissue damage. Moreover, less accurate insertion is associated with more tissue damage, since the insertion must be repeated. The friction force between needle and tissue has the biggest contribution to ultimate insertion force, and it equals to the extraction force; therefore, decreasing the friction force will reduce both insertion and extraction forces of the needle.

To generate a novel needle design, the insertion mechanics of insect stingers have been studied Researchers such as Ling et al. [19] and Cho [20] showed that barbs in honeybee stinger reduce its insertion force significantly. Ling et al. [19] reported that the average insertion force of the honeybee stinger is 5.75 mN, which is about one order of magnitude smaller than that of an acupuncture microneedle. They concluded that barbs reduce the friction force of needle which leads to a significant reduction in the insertion force of honeybee stinger. On the other hand, the average extraction force was about four times larger than that of the acupuncture microneedle. The extraction force was increased due to the mechanical interlocking of the barbs to the tissue.

In our previous work [21–24], a new design for barbs was generated which preserved the advantages of barbs in honeybee stinger (including their low penetration and in-

* *Corresponding author*
Assoc. Prof. Parsaoran Hutapea, e-mail: hutapea@temple.edu

sertion forces), and removes and reduces their disadvantages (such as high extraction force and asymmetric geometry). In our design [21–23, 25, 26], barbs were carved on needles body to avoid any increase in the extraction force; moreover, they were symmetric which means there would not be any unbalanced normal force acting on needles surface during insertion. Unbalanced normal forces can increase the needle deflection and deviate needle from its target.

The insertion and extraction tests into artificial (tissue-mimicking PVC gel) and biological (bovine liver and brain) tissues were performed using bioinspired and conventional needles to investigate the effectiveness of the new needle design. The results showed that the bioinspired needle reduces the insertion force by 25–46%, and extraction force by 20–25% [21–23, 25]. The scale study was conducted to investigate the size effect on bioinspired needle performance. The insertion tests into PVC gels and bovine liver tissue were performed using bioinspired and conventional needles in five different scales. The scale study results showed 20–28% reduction in insertion forces in insertion into PVC gels, and 46% reduction in insertion into bovine liver tissue using bioinspired needles.

The reduction in needle forces is conjectured to reduce the tissue deformation during the medical procedure. It has been observed by different researchers that reducing tissue deformation will improve needle's placement accuracy and decrease tissue damage [5]. This hypothesis has been investigated in our latest published work [27], in which digital image correlation was utilized to measure tissue deformation during insertion. The DIC results showed 17% reduction in tissue deformation using bioinspired needle.

In this paper, a histological study was conducted to accurately measure the tissue damage caused by insertion of bioinspired and conventional needles. The insertion and extraction tests of both bioinspired and conventional needles were performed using bovine liver tissue. Small samples of the liver tissue around injection spot were cut, trimmed, and fixed. The samples were sectioned into slices with the thickness of 0.08 ìm using a microtome machine. The previously sectioned and mounted tissues were stained using hematoxylin and eosin (H and E) staining method to improve visualization of the cells. The needle insertion area was located on the slide and were using an Olympus CKX53 Inverted Microscope equipped with an Olympus Color Camera DP22. Image J was used to stitch the snapshots taken together to provide a full image of the needle insertion, and to measure the cross-sectional area of the needles' paths. The damaged cross-sectional area due to the insertion of conventional and bioinspired needles were 100735 Pixels and 69657 Pixels, respectively. By comparing two damaged cross-sectional areas, it can be concluded that the damage caused by needles into bovine liver tissue decreased by 31% using bioinspired needle.

2. Material and methods

2.1. Bioinspired needle design and insertion setup

A barb design inspired by barbs in honeybee stinger were generated (Fig. 1a). In our barb design, the advantages of the barbs in honeybee stinger were preserved, and its disadvantages were removed or reduced. When it comes to using barbs in a needle design, the extraction force of needle is a concern. However, in our design, barbs are carved on needle body (Fig. 1b), so that they do not increase the cross-sectional area of the needle and its cutting force in insertion; the extraction tests were performed to validate this hypothesis, and it has been shown that barbs do not increase the extraction force.

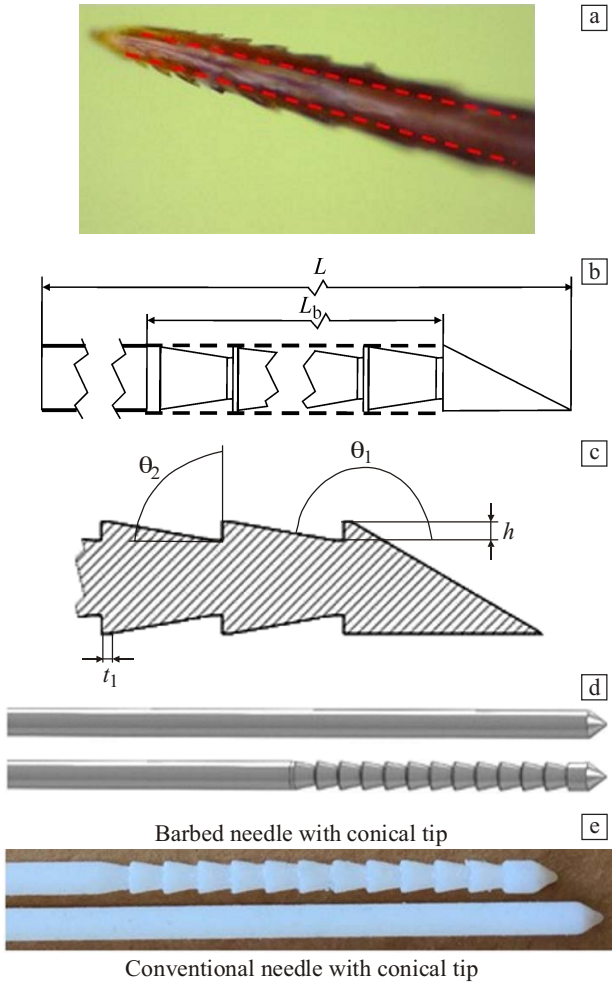

Fig. 1. (a) Honeybee stinger (barbs are coming out of the stinger body), (b) design of the barbs in bioinspired needle (barbs are carved on needle's body) (L is the length of the needle, and L_b is the length of the barbed section), (d) design parameters of the barbs, barb's front angle θ_1, barb's back angle θ_2, barb height h, and thickness of the barb tip t_1 (20), (e) 3D models of the bioinspired and conventional needles, and (f) 3D printed needles.

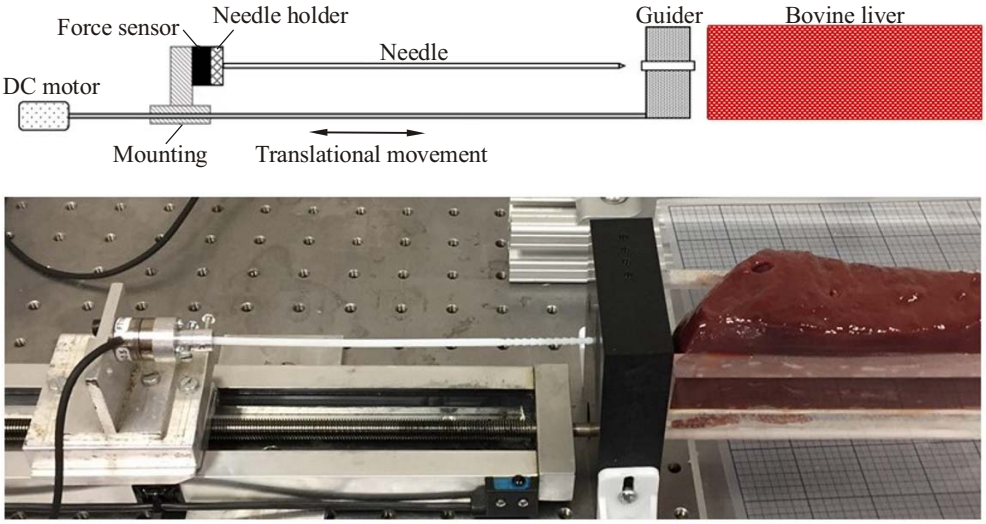

Fig. 2. Experimental setup.

Having symmetricity in needle design is crucial for mesoscale needles(ranging from 0.1 to 5.0 mm, which includes surgical needles such as hypodermic and biopsy needles); this is because any asymmetric section in a needle will generate forces on the needle body, which causes the needle to bend and deviate it from its target. In an axisymmetric needle, the forces acting on the needle body cancel each other out. Having less or no normal forces acting on the body is always desirable and helps us to control the needle path inside the tissue easier. The manufacturability of a symmetric design is also higher than an asymmetric design due to the simplicity of barb geometry.

The design parameters of the barbs are the front θ_1 and back θ_2 angles of the barb, barb height h, barb tip thickness (which indicates the sharpness of the barb tip) t_1, and the length of the section with barbs L_b. The length of the section with barbs L_b is shown in Fig. 1b, and the rest of the parameters are illustrated in Fig. 1c.

Three-dimensional models of bioinspired and conventional needles were generated using Solidworks as illustrated in Fig. 1d. The models were saved as STL files and manufactured using a Connex350 3D printer (Stratasys, Inc., Eden Prairie, MN), as shown in Fig. 1e. The Connex350 3D printer has a high-resolution print layer accuracy of 16 μm.

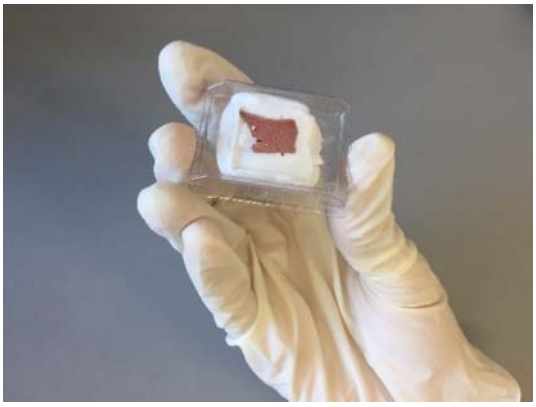

Fig. 3. A fixed liver sample.

Multiple needles insertions and extractions were performed into bovine liver tissue using bioinspired and conventional needle. The experimental setup included a linear motor to provide translational motion, a force sensor, a programmable data acquisition system to record the insertion force, and a bovine liver tissue (see Fig. 2). The force sensor was a six-axis Force/Torque Transducer Nano17® (ATI Industrial Automation, Apex, NC).

2.2. Samples preparation for histological study

First, the insertion and extraction tests of both bioinspired and conventional needles were performed using bovine liver tissue. Then, small samples of the liver tissue around needles paths were cut and trimmed. Samples were immersed in 4% formaldehyde and left there for one day. Next, samples were taken out from the 4% formaldehyde solution, and a sucrose with 30% (w/v) was added to them. The samples were cut into 5mm thickness slices, optical cutting temperature (OCT) was added to them and they were placed into cryomolds. The samples were frozen completely for two days in a –80°C refrigerator (Fig. 3). Those samples were sectioned into slices with the thickness of 0.08 ìm using a microtome machine (Fig. 4). These sectioned slices were attached to micro slides and kept on a slide warmer at a temperature of 20–25°C.

2.3. Hematoxylin and Eosin staining

Hematoxylin solution, Eosin Y solution, and xylene were purchased from Sigma-Aldrich Co., and permount Mounting Medium and ethanol were purchased form Fisher Scientific. Tissue-Tek dishes were washed thoroughly and la-

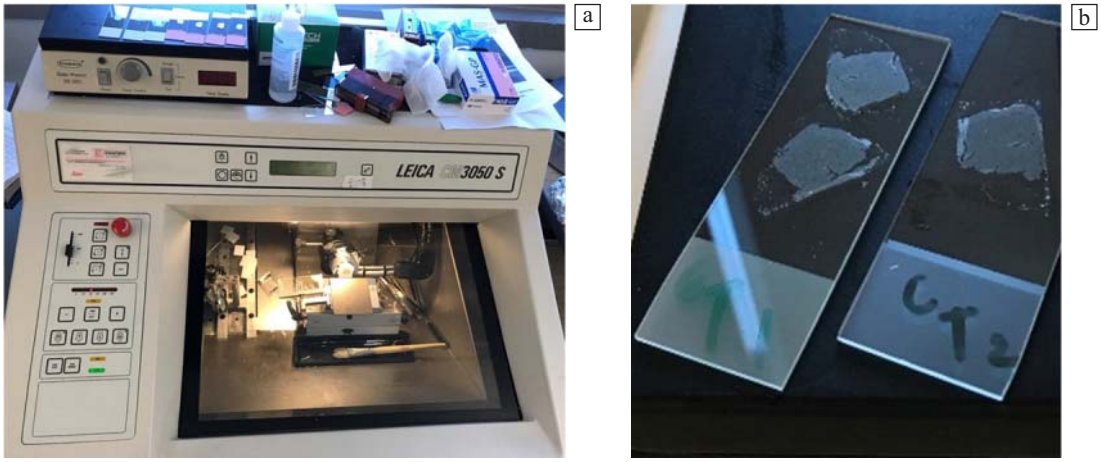

Fig. 4. (a) The microtome machine used to section fixed liver samples, and (b) the sectioned slices with thickness of 0.8 μm.

beled according to the intended solution. For a Hematoxylin and Eosin (H and E) stain, graded ethanol for 70 to 100% was made by diluting 100% ethanol with DI water to obtain the desired % (v/v) concentration. Hematoxylin solution, Eosin Y solution, xylene, and the as-prepared ethanol solutions were added to a Tissue-Tek dish. The solutions were filled to the top line to allow for complete submersion of the slides. Slides with sliced tissue were added to a Tissue-Tek slide holder in preparation for each staining step.

The previously sectioned and mounted tissues were dehydrated by soaking the slides (5 min) in xylene and 50:50 xylene: ethanol. The specimens were then soaked for 5 min each in graded alcohols from 70 to 100% for dehydration. Next, the slides were added to 10% (v/v) hematoxylin in water for 5 min and washed 2x with tap water. The slides were then added to 1% (v/v) eosin y in water for 20 s then washed 2x in tap water. Samples were then rehydrated using graded alcohols from 100 to 70% and xylene for 5 min.

2.4. Coverslip mounting

The slides from 2.4 were allowed to air dry for 10 min. Three 100 μL drops of permount were placed on each slide. Then coverslips were added to the slides and pressure was applied until the excess permount leaked out the sides of the slide. A Kimwipe was used to wipe the excess mounting solution then nail polish was used to seal the slide.

2.5. Imaging

An Olympus CKX53 Inverted Microscope equipped with an Olympus Color Camera DP22 was used to image the stained slides. The slides were placed face up on the microscope and imaged at 4x magnification. The exposure time was set to 10 ms and kept constant through the duration of the imaging. The manual brightness was kept the same throughout the imaging process. The needle insertion area was located on the slide and images were taken of the surrounding areas. Image J was used to stitch the snapshots taken from 2.5 together to provide a full image of the needle insertion (Fig. 5).

3. Results

Figure 6 shows the damages caused by the bioinspired and conventional needles into bovine liver tissue. Using ImageJ software, the cross-sectional area of the needles' paths were measured. The damaged cross-sectional area due to the insertion of conventional and bioinspired needles were 100735 Pixel and 69657 Pixel, respectively. By comparing two damaged cross-sectional areas, it can be concluded that the damage due to the insertion and extraction of the needle into bovine liver tissue decreased by 31% using a bioinspired needle. The results obtained from the histological study are in agreement with our hypothesis that reducing needle's forces and tissue deformation during insertion leads to less invasive needle-based procedures.

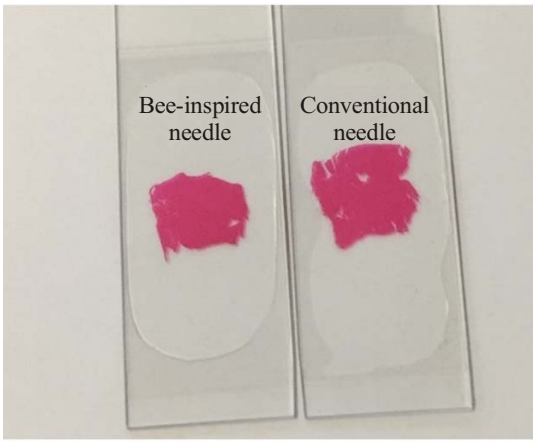

Fig. 5. The sectioned liver samples after Hematoxylin and Eosin (H and E) staining.

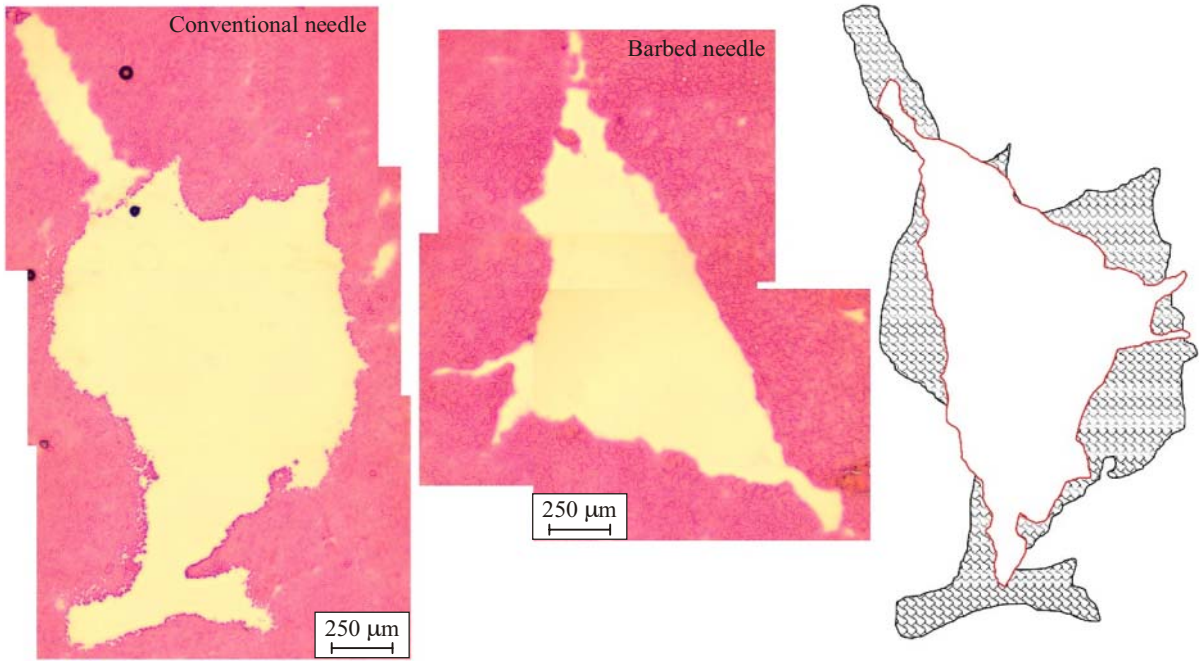

Fig. 6. Damages caused by insertions of bioinspired and conventional needles into bovine liver tissue.

4. Conclusions

A histological study was conducted to accurately estimate the tissue damage caused by the bioinspired and conventional needle. The results of the histological study showed that the damage due to the insertion and extraction of the needle into bovine liver tissue decreased by 31% using a bioinspired needle. The proposed bioinspired needle design has been shown to significantly reduce the insertion and extraction forces of the needle, and its damage to tissue. Using a bioinspired needle, the tissue deformation was decreased which improved the insertion accuracy. The histological study result is in agreement with our hypothesis that reducing needle's forces and tissue deformation leads to less invasive percutaneous procedures.

As future work, the effect of bioinspired needles on targeting accuracy can be investigated through multiple insertion tests. The deflection of the bioinspired needle during insertion can be studied using an implantable elastomeric polymeric magnet and a giant magnetoresistance sensor. Using data obtained from this study, the deflection of the bioinspired needle can be predicted based on barb design parameters using machine learning. Furthermore, available manufacturing methods (such as laser cut, mesoscale manufacturing, and metal three-dimensional printing) can be explored to see which method can be implemented to manufacture bioinspired needles. Finally, the potential medical and industrial applications of bioinspired needle design should be explored. Since the new design decreases the tissue damage significantly, it can be implemented to design needles, electrodes, and leads which used inside fragile tissues such as brain and liver tissue. The bioinspired design also reduces tissue deformation during insertion, this feature can be essential in procedures like brachytherapy or tumor ablation. The design can be implemented to develop novel soil nails which used to reinforce the ground in nailing technique.

Acknowledgments

Authors would like to acknowledge Dr. M.F. Kiani from the Department of Mechanical Engineering at Temple University for letting us use the Microtome machine in the Biofluidics Laboratory to section our samples. We would like to thank the Department of Bioengineering at Temple University for providing us the materials used to fix and stain the samples, and the microscope for obtaining take sample images.

References

1. Okamura AM, Simone C, O'Leary MD. Force modeling for needle insertion into soft tissue. IEEE Trans Biomed Eng. 2004; 51: 1707–1716.
2. Shergold O, Fleck N. Experimental investigation into the deep penetration of soft solids by sharp and blunt punches, with application to the piercing of skin. J Biomech Eng. 2005; 127: 838–848.
3. Chebolu A, Mallimoggala A, Nagahanumaiah: Modelling of cutting force and deflection of medical needles with different tip geometries. Proc Mater Sci. 2014; 5: 2023–2031.
4. Abolhassani N, Patel R, Moallem M. Control of soft tissue deformation during robotic needle insertion. Minim Invasive Ther Allied Technol. 2006; 15: 165–76.
5. van Gerwen DJ, Dankelman J, van den Dobbelsteen JJ. Needle-tissue interaction forces—A survey of experimental data. Med Eng Phys. 2012; 34: 665–680.

6. Meltsner MA, Ferrier NJ, Thomadsen BR. Observations on rotating needle insertions using a brachytherapy robot. Phys Med Biol. 2007; 52: 6027–6037.
7. Misra S, Reed KB, Douglas AS, Ramesh KT, Okamura AM. Needle-tissue interaction forces for bevel-tip steerable needles. In: Proc 2nd Bienn IEEE/RAS-EMBS Int Conf Biomed Robot Biomechatronics; 2008.
8. Henley DE, Leendertz JA, Russell GM, Wood SA, Taheri S, Woltersdorf WW, Lightman SL. Development of an automated blood sampling system for use in humans. J Med Eng Technol J J Med Eng Technol. 2009; 333: 309–1902.
9. Brett PN, Harrison AJ, Thomas TA. Schemes for the identification of tissue types and boundaries at the tool point for surgical needles. IEEE Trans Inf Technol Biomed. 2000; 4: 30–36.
10. Esmaeili Pourfarhangi K, Sahlabadi M. The size of red blood cells regulates the extent of pulmonary capillary diameter effect on pulmonary gas exchange process. 2017.
11. Powell S, How TV, Groves D, Hatfield F, Diaz BM, Gould D. *In vivo* force during arterial interventional radiology needle puncture procedures. Stud Health Technol Inform. 2005; 111: 178–184.
12. Crouch JR, Schneider CM, Wainer J, Okamura AM. A velocity-dependent model for needle insertion in soft tissue. Lect Notes Comput Sci (including Subser. Lect. Notes Artif. Intell. Lect. Notes Bioinformatics). 2005; 3750 LNCS: 624–632.
13. Crouch JR, Schneider CM, Wainer J, Okamura AM. Needle insertion with tissue relaxation. Cs Odu Edu; 2005.
14. Urrea FA, Casanova F, Orozco GA, García JJ. Evaluation of the friction coefficient, the radial stress, and the damage work during needle insertions into agarose gels. J Mech Behav Biomed Mater. 2016; 56: 98–105.
15. DiMaio SP, Salcudean SE. Needle insertion modeling and simulation. Ieee Trans Robot Autom. 2003; 19: 864–875.
16. Abolhassani N, Patel RV, Ayazi F. Minimization of needle deflection in robot-assisted percutaneous therapy. Int J Med Robot Comput Assist Surg. 2007; 3: 140–148.
17. Mahvash M, Dupont PE. Fast needle insertion to minimize tissue deformation and damage. In: Proc IEEE Int Conf Robot Autom; 2009.
18. Mahvash M, Dupont PE. Mechanics of dynamic needle insertion into a biological material. IEEE Trans Biomed Eng. 2010; 57: 934–943.
19. Ling J, Song Z, Wang J, Chen K, Li J, Xu S, Ren L, Chen Z, Jin D, Jiang L. Effect of honeybee stinger and its microstructured barbs on insertion and pull force. J Mech Behav Biomed Mater. 2017; 68: 173–179.
20. Cho WK, Ankrum J, Guo D, Chester S, Yang SY, Kashyap A, Campbell G, Wood RJ, Rijal RK, Karnik R, Langer R, Karp JM. Microstructured barbs on the North American porcupine quill enable easy tissue penetration and difficult removal. Proc Natl Acad Sci USA. 2012; 109: 21289–21294.
21. Sahlabadi M, Gardell D, Attia JS, Khodaei S, Hutapea P. Insertion mechanics of 3D printed honey-bee-inspired needle prototypes for percutaneous procedure. In: Design of medical devices. Minneapolis, Minnesota; 2017.
22. Sahlabadi M, Khodaei S, Jezler K. Insertion mechanics of bioinspired needles into soft tissues. Minim Invasive Ther Allied Technol. 2017; 0: 1–8.
23. Sahlabadi M, Khodaei S, Jezler K, Hutapea P. Study of bioinspired surgery needle advancing in soft tissues. In: Proceedings of the ASME 2017 Conference on Smart Materials, Adaptive Structures and Intelligent Systems SMASIS2017; 2017.
24. Khodaei S, Sahlabadi M, Hutapea P. Design of smart barb of honeybee-inspired surgery needle seyedvahid. In: Proceedings of the ASME 2017 Conference on Smart Materials, Adaptive Structures and Intelligent Systems SMASIS2017; 2017.
25. Sahlabadi M, Hutapea P. Novel design of honeybee-inspired needles for percutaneous procedure. Bioinspir Biomim. 2018; 13: 036013, 1–16.
26. Sahlabadi M. A novel bioinspired design for surgical needles to reduce tissue damage in interventional procedures; 2018. Available from: https://search.proquest.com/docview/2046858179?accountid=14270
27. Sahlabadi M, Hutapea P. Tissue deformation and insertion force of bee-stinger inspired surgical needles. J Med Device. 2018; 1–12.